Wet Steam Conference, Prague
September 12–14 2016

Results of the International Wet Steam Modelling Project

Jörg Starzmann*, Fiona R. Hughes and Alexander J. White
Hopkinson Laboratory, University of Cambridge, United Kingdom.
*Corresponding author: Email: js2145@cam.ac.uk or ajw36@cam.ac.uk

Jan Halama, Vladimir Hric and Michal Kolovratník
Czech Technical University Prague, Czech Republic.

Hoon Lee
Doosan Heavy Industry & Construction, South Korea.

Libor Sova and Miroslav Šťastný
Doosan Skoda Power and West Bohemia University, Czech Republic.

Sebastian Schuster
Chair for Turbomachinery, Universität Duisburg-Essen, Germany.

Marius Grübel, Markus Schatz and Damian M. Vogt
Institute for Thermal Turbomachinery and Machinery Laboratory, Universität Stuttgart, Germany.

Yogini Patel, Giteshkumar Patel and Teemu Turunen-Saaresti
Lappeenranta University of Technology, Finland.

Vladimir Gribin, Victor Tishchenko and Ilya Gavrilov
Moscow Power Engineering Institute, Russia.

Changhyun Kim and Jehyun Baek
POSTECH, Pohang University of Science and Technology, South Korea.

Xiaoming Wu and Jiandao Yang
Shanghai Turbine Works Co. Ltd., China.

Sławomir Dykas and Włodzimierz Wróblewski
Silesian University of Technology, Poland.

Satoru Yamamoto
Tohoku University, Japan.

Zhenping Feng and Liang Li
Xi'an Jiaotong University, China.

Abstract

The purpose of the "International Wet Steam Modelling Project" is to review the ability of computational methods to predict condensing steam flows. The results of numerous wet-steam methods are compared with each other and with experimental data for several nozzle test cases.

The spread of computed results is quite noticeable and the present paper endeavours to explain some of the reasons for this. Generally, however, the results confirm that reasonable agreement with experiment is obtained by using classical homogeneous nucleation theory corrected for non-isothermal effects, combined with Young's droplet growth model. Some calibration of the latter is however required. The equation of state is also shown to have a significant impact on the location of the Wilson point, thus adding to the uncertainty surrounding the condensation theory.

With respect to the validation of wet-steam models it is shown that some of the commonly used nozzle test cases have design deficiencies which are particularly apparent in the context of two- and three-dimensional computations. In particular, it is difficult to separate out condensation phenomena from boundary layer effects unless the nozzle geometry is carefully designed to provide near-1D flow.

It is hoped that this study will prove useful to the participants in showing how their methods compare with others. It is also hoped that it will provide a basis for improvements to the various modelling approaches.

Keywords wet-steam, nozzle, nucleation, droplet growth

1 Introduction

In steam turbines the formation of wetness causes additional dissipation, blade erosion and corrosion problems. Many publications are dedicated to this subject and it is hard to single out any one of these as they range from experimental to entirely theoretical investigations, and from simplified one-dimensional approaches to studies of real turbine applications. The latest wet-steam special issues (Bakhtar, 2004, 2005; Young and White, 2014) provide a comprehensive overview of past research along with more recent developments.

Computational Fluid Dynamics (CFD) was firmly established in the field of turbomachinery by the end of the last century and it now also dominates wet-steam research in terms of numbers of papers. Modern wet-steam numerical methods are usually based on the theories of droplet formation and growth in the context of a thermodynamically non-equilibrium flow environment, but there is a wide range of approaches in terms of how the models are implemented. In 2015 the "International Wet Steam Modelling Project" (IWSMP) was initiated to examine the current state of fundamental wet-steam modelling within modern CFD methods. For this purpose institutions and companies were invited to provide flow calculations for a few well-known validation nozzle tests. This paper presents the outcome of this collaboration and includes results from all participants.

The motivation for the IWSMP arose from the fact that, within the wet-steam community, different condensation models and various numerical methods are used but, surprisingly, no common modelling standard has emerged over the years. In order to validate nucleation and droplet growth theories it has been most convenient to use experimental data from supersonic nozzle flows, such as those described by Barschdorff (1971); Young (1982); Wróblewski et al. (2009). Most researchers manage to achieve reasonable (or even excellent) agreement for one or two nozzles, but matching computation and experiment for the entire range of test cases has proved elusive. Uncertainties persist regarding the numerical methods, the fundamental theories of nucleation and droplet growth, and indeed some of the experimental data. One may conclude that this is a rather unsatisfactory situation, which has now been going on for some thirty years, but it is also true to say that spontaneous condensation is a complicated process that is exceptionally sensitive to small changes in various physical quantities.

Since the earliest attempts to match theory with nozzle experiments, one of the main changes has been the advent of multi-dimensional CFD methods. This has revealed a host of additional uncertainties and called into question the suitability of some of the experiments. The authors believe that this situation justifies a review of the current status of wet-steam modelling, the particular aim at this stage being to clarify the influence of different numerical methods, model assumptions and their implementation. This is the first time that the majority of worldwide wet-steam methods has been assembled for comparison on a common basis, and this is perhaps one of the main achievements of this collaboration. It is hoped that the results of this project will provide a starting point for future endeavours of similar nature, perhaps eventually leading to the establishment of some recommended procedures (and test cases) for code validation, as well as agreement as to the best combination of modelling approaches to adopt.

In the following sections a short explanation of condensing nozzle flows is first given before the IWSMP is introduced in more detail. Subsequently the numerical results from the project participants are compared with each other and with experimental data. The influence of various modifications to the nucleation and droplet growth models as well as the effect of different

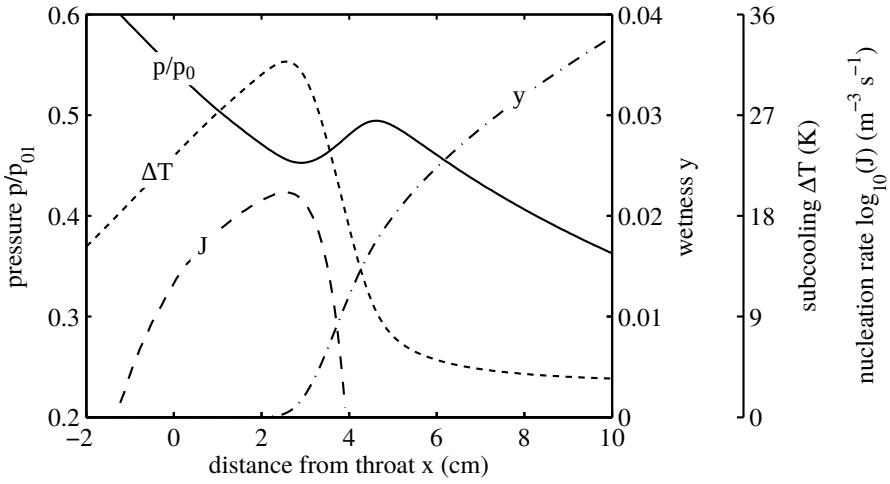

Fig. 1: Typical result of a stationary condensing nozzle flow for given inlet conditions

numerical methods is then investigated. Finally, tentative recommendations are made for undertaking nozzle calculations and suggestions are given for further work.

2 Condensing nozzle flows

The initial validation of wet-steam methods relies heavily on experimental data obtained from condensing nozzle flows, chiefly because the flow in such nozzles is much simpler than that within a turbine. Well-designed nozzles can produce a steady, near-1D flow that nonetheless replicates the expansion rate, Mach number and subcooling conditions that are encountered in real turbines. Although most readers will no doubt be familiar with condensing nozzle flow, we give a brief outline of the main phenomena in order to draw attention to some of the particular issues relating to the validation of numerical methods.

Fig. 1 shows typical variations in key quantities for flow in a converging-diverging nozzle. The steam is accelerated in the nozzle and the pressure falls in accord with supersonic expansion in the diverging section. As is well known, non-equilibrium conditions are established due to the Gibbs free energy barrier associated with droplet formation, and thus condensation only commences once the steam is subcooled, typically by some 30 K. For an initially dry stagnation state this will normally be downstream of the throat where the flow is supersonic. The nucleation rate rises extremely rapidly with subcooling and at some point enough nuclei are present to support appreciable condensation. In adiabatic flow the latent heat release is absorbed by the vapour, raising its temperature and bringing the flow back towards equilibrium. The point of maximum subcooling is called the Wilson point and, for given inlet conditions, its location depends on the expansion rate, as quantified by $\dot{P} = -\mathrm{d}(\ln p)/\mathrm{d}t$. (Note that the cooling rate $-\mathrm{d}T/\mathrm{d}t$ is more commonly used for moist air flows.)

The heat release affects all the flow properties and in particular the characteristic pressure rise (sometimes misleadingly referred to as the ‘condensation shock’) is used to compare experiment and theory. The location and shape of this pressure rise is determined by both the rate of formation of droplets (i.e., the nucleation rate) and by their subsequent growth rate. These two processes are intimately linked – for example, an increase in the droplet growth rate causes a more rapid reduction in subcooling, thereby quenching nucleation earlier and resulting in fewer, but larger droplets. As pointed out by Young (1982), it is therefore important to match both the pressure distribution and the droplet size in order to properly validate wet-steam models.

It is obvious that a reduction in inlet temperature causes the condensation to move upstream within the nozzle. The pressure rise becomes steeper as a consequence of heat release taking place closer to sonic conditions and eventually a true, aerodynamic shockwave becomes embedded within the condensation zone. Further reduction in inlet temperature results in self-excited

oscillations, detailed studies of which have been undertaken by Schnerr (2005) (especially for moist air flows) and others. Although these oscillatory regimes are of considerable scientific interest and may well be of practical relevance to turbine flows, they are perhaps less important for initial validation studies and have not been included in the present project.

3 Project overview

Thirteen research groups have taken part in this collaboration and contributed their numerical results. In order to achieve an unbiased comparison between the different methods, structured grids (coarse, medium, fine) were provided to the participants. Node numbers and the spatial extent of these are given in Table A1 of the appendix. All grids were refined in the expected condensation zone and near the walls. In addition to fully 3D grids that resolve the boundary layers of all four walls, grids for 2D calculations were also made available. A grid-independent solution in terms of pressure can often be reached with the coarsest grid, whereas convergence for the droplet size typically requires finer resolution. Nonetheless, most participants achieved reasonably grid-independent solutions with the medium grids. DoSkoda's method is an unstructured solver and they thus undertook their own meshing. The numbers of nodes required to give grid-independent solutions in their case is also given in Table A1.

Participants were completely free in their choice of numerical and wet-steam models. An overview of the different approaches is provided in Table A2 of the appendix, together with details of the participating institutions. Despite the variations, there are a number of common themes that are worth noting:

1. Most, but not all, of the solvers are in-house "high-order" finite-volume methods.
2. Standard turbulence models were generally applied, although several solvers were restricted to laminar flow and in some cases participants assumed laminar flow for a specific test case.
3. No inlet boundary layer profiles have been specified by the participants.
4. Classical nucleation theory has been universally adopted, with or without Kantrowitz's non-isothermal correction (as described in Sec. 7.3).
5. More variation is to be found in droplet growth modelling, but most used Young's equation (see Sec. 7.4) albeit with different model parameters.
6. The most common approach for modelling the droplet spectra was to assume a single, mean droplet size (i.e., monodispersed), but moment methods and one polydispersed model were also used.
7. Equations of state ranged from simple ideal gas relations through virial equations to the Gibbs-based IAPWS-IF97 formulation.

In addition to the above, Table A2 also lists the various relations used for additional properties such as viscosity, conductivity, surface tension, latent heat and liquid density. With the exception of Tohoku, all participants calculated the different test cases with consistent model settings.

The selected test cases were Moore et al. (1973) nozzle B and the Moses and Stein (1978) nozzle at two different inlet conditions. These nozzles were chosen because both pressure and mean droplet size data are available in the literature. (Note that steady nozzle flows yield narrow droplet size spectra (see for example Bakhtar et al., 2005) so an average size measurement is all that can usually be obtained.) However, both nozzles have features that render them less than perfect for validation purposes (see discussion in Sec. 4 and 5) and so an additional "Mystery" nozzle geometry was developed. The lack of experimental data for this geometry is clearly a drawback, but it does nonetheless have the advantage of providing a (permanently) "blind" test case.

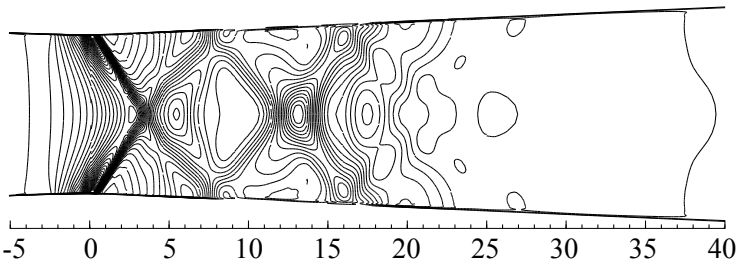

Fig. 2: Isolines of the density gradient for the Moore nozzle B, calculated with the 3D laminar CAM model

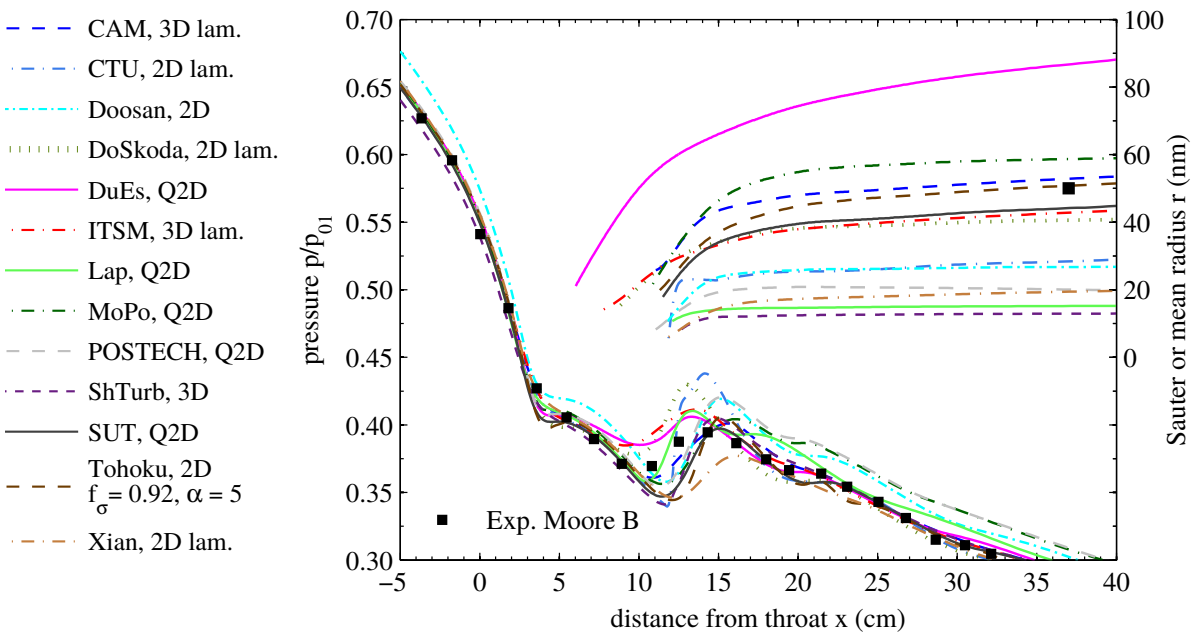

Fig. 3: Pressure and droplet radius for Moore nozzle B, $p_{01} = 25\,\mathrm{kPa}$ and $T_{01} = 358.1\,\mathrm{K}$

4 Moore nozzle B test case

Moore et al. (1973) investigated a series of nozzle designs with various expansion rates. Amongst these, nozzle B has relatively large throat dimensions of $0.1 \times 0.152\,\mathrm{m}$ (height $\times$ depth) and provides an expansion rate of around $2300\,\mathrm{s}^{-1}$ shortly after the throat. Pressure measurements were conducted using wall-tappings on the plane side-wall along the centre line and the Sauter mean droplet radius, also on the centre line, was obtained near the outlet using the light extinction method of Walters (1973). The test was undertaken with inlet stagnation conditions of $p_{01} = 25\,\mathrm{kPa}$ and $T_{01} = 358.1\,\mathrm{K}$. This resulted in a relatively low Wilson point pressure of about $10\,\mathrm{kPa}$.

Before analysing the results obtained, a few comments are in order regarding this commonly used but partly unsatisfactory nozzle. The wall profile consists of a curved inlet section (converging part) that blends with a straight diverging section downstream of the throat. Unfortunately, the geometry of the inlet is not fully specified in Moore et al. (1973) and hence for the present purposes it has been designed to match the measured pressure distribution upstream of the throat. A significant drawback of all the Moore et al. nozzles is that the curvature discontinuity at the profile blend point generates a series of expansion and compression waves. As shown in Fig. 2, these are reflected by the opposite walls, resulting in pressure undulations along the nozzle centre line that potentially interfere with the condensation zone. As discussed by Starzmann et al. (2016), the presence of these strong two-dimensional features also means that, despite of the size of the nozzles, the flow is significantly affected by boundary layer growth. (The boundary layer on the curved walls influence the emanating expansion fan and the boundary layer on the plane side-walls serve to smooth the effective wall pressure profile.)

Fig. 3 shows numerical results from all the project members together with measured data. Although analysing such a crowded plot is difficult, it does at least provide an overview of the scatter and trends of the different results. Considering the distribution of both pressure and droplet radius, it can be seen that the models of DoSkoda, DuEs and ITSM predict nucleation rather early. DoSkoda uses classical nucleation theory without the non-isothermal correction whereas DuEs reduces the planar surface tension by 5% (see Tab. A2), which in both cases results in high nucleation rates. It is not obvious why the ITSM model also predicts condensation early, but some further discussion is offered in Sec. 7.2. In order to match pressures Tohoku also reduced surface tension relative to the flat-film value (in this case by 8%), which, as discussed in Sec. 7.3 typically increases nucleation by a factor of 1000. (In fact, Tohoku modifies the surface tension and Young's droplet growth parameter α independently for each test case and this should be borne in mind when interpreting the level of agreement.)

Most models predict a steeper condensation pressure rise than observed in the experiment. This may well be due to the nucleation and growth models adopted, but Starzmann et al. (2016) showed that, due to the above-described pressure undulations, the pressure distribution at the wall is sensitive to the state of the boundary layer. (It was shown that a 3D laminar calculation, resolving the boundary layers on all four walls, prevents the condensation pressure rise overshooting the measured values.) The shape of the pressure rise is however in good agreement with measurements for the results of CAM and Xian, although in Xian's case it is predicted too far downstream. (This is despite Xian's use of an artificially high condensation coefficient, $q_c = 100$, which increases both droplet growth and especially the nucleation rate.)

Several of the methods over-predict the pressure in the region downstream of the condensation zone, but it is not yet clear why this should be so. However, the following observations may be made: (i) In some cases (e.g., Lap) the discrepancy is quite small and localised and may be due to the sensitivity of the expansion/compression waves modelling to the boundary layers; (ii) As well as over-predicting pressure in the downstream region, Doosan's method also shows significant discrepancies in the inlet, well upstream of condensation; (iii) The results of POSTECH consistently over-predict pressures in the downstream regions for most of the test cases.

Once account is taken of an measurement accuracy of perhaps $\pm 20\%$ only one method (DuEs) significantly over-predicts the droplet size, whereas several result in droplets that are too small. The tendency to under-predict droplet sizes at low Wilson point pressures is discussed by Young (1982) whose growth law consequently includes the parameter α which, although justifiable on the basis of a plausible physical argument, provides a tunable, empirical factor. As described in Sec. 7.4, higher values of α serve to boost the growth rate, thus resulting in larger droplets whilst simultaneously shifting the pressure rise upstream and bringing it into closer agreement with the experiments. (By contrast, increasing the nucleation rate moves the pressure rise upstream but reduces the final droplet size.)

In summary, the strong two-dimensional flow structures for the Moore nozzle detract from its suitability for validation of wet-steam models. Nevertheless the results show that reasonably good agreement with the experimental data is obtained with at least some of the methods, and all methods produce results that are broadly correct in terms of the qualitative flow features.

5 Moses and Stein nozzle test cases

The Moses and Stein (1978) nozzle is much smaller than that of Moore et al. and hence the expansion rate near the throat is about $6500\,\mathrm{s}^{-1}$ and in the condensation zone it is between $9000\,\mathrm{s}^{-1}$ and $10\,000\,\mathrm{s}^{-1}$. The geometry is given in Moses and Stein (1978) and consists of two arcs with different radii. Unfortunately the point where the arc radius changes from 5.3 cm to 68.6 cm is not explicitly given but can be estimated from one of the figures in the paper. The smoother wall profile means that this nozzle is relatively free from undesirable pressure undulations, but the small throat dimensions (10 mm by 10 mm) suggest that boundary layer blockage may be significant.

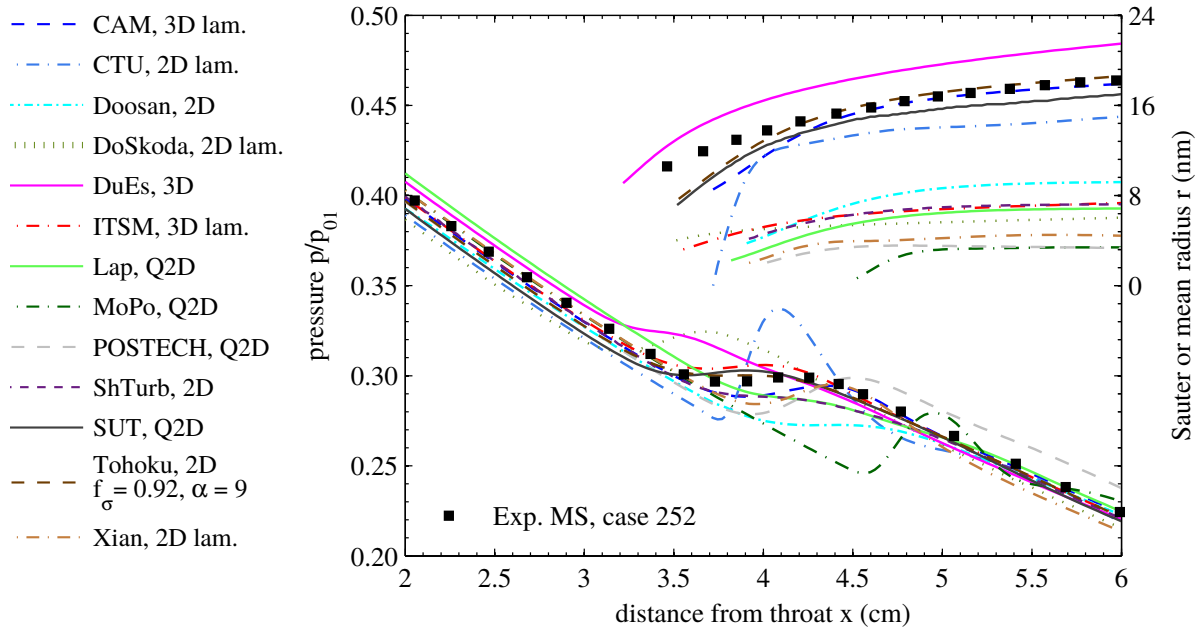

Fig. 4: Moses and Stein nozzle, case 252, $p_{01} = 40.05\,\mathrm{kPa}$ and $T_{01} = 374.3\,\mathrm{K}$

Test cases 252 and 257 are considered within the IWSMP, providing Wilson point pressures of about 12 kPa and 25 kPa respectively. Pressure measurements are available along the nozzle centre line and a light-scattering method was used to obtain droplet size data. Light scattering curves for case 252 are given in the Moses and Stein paper and have been processed by Young (1982). The experimental data for case 257 are not included in the original paper and were obtained from Guha and Young (1991).

5.1 Comparison of experimental and numerical results for test 252

Fig. 4 shows the results for case 252 at the lower Wilson point pressure. Firstly, it is notable that even upstream of condensation the numerical results clearly differ from each other. As discussed by Starzmann et al. (2016) the nozzle throat is small enough that boundary layer blockage noticeably influences the mass flow rate and the static pressure distribution. In broad terms, 2D laminar calculations tend to under-predict the upstream pressure, 3D laminar and 2D turbulent models give reasonable agreement with experiment, whilst for 3D turbulent models the upstream pressure is too high. These findings suggest that laminar-turbulent boundary-layer transition may be occurring downstream of the throat.

As with the previous test case, CTU over-predicts the condensation pressure rise whilst DuEs and DoSkoda estimate condensation too far upstream. The model of MoPo determines the Wilson point considerably too far downstream and under-estimates the droplet size. Doosan also predicts the pressure rise late but is using Gyarmathy's growth law which results in lower growth rates than Young's model (see Sec. 7.4). The closest agreement with the measured pressure rise is obtained by SUT and ITSM, but the former gives pressures that are too low in the upstream section whilst the latter produces droplets that are too small. In fact, again in common with the previous test case, there is a general tendency to under-predict droplet sizes even if a measurement uncertainty of 20% is assumed.

5.2 Comparison of experimental and numerical results for test 257

It is of course desirable to validate the models over a broad pressure range because even in low pressure turbines it is possible for Wilson point pressures to vary between 10 kPa and maybe 100 kPa. Unfortunately there is a dearth of good quality data at higher pressures, but test 257 does at least give a Wilson point of around 25 kPa. For this case the ITSM calculation now

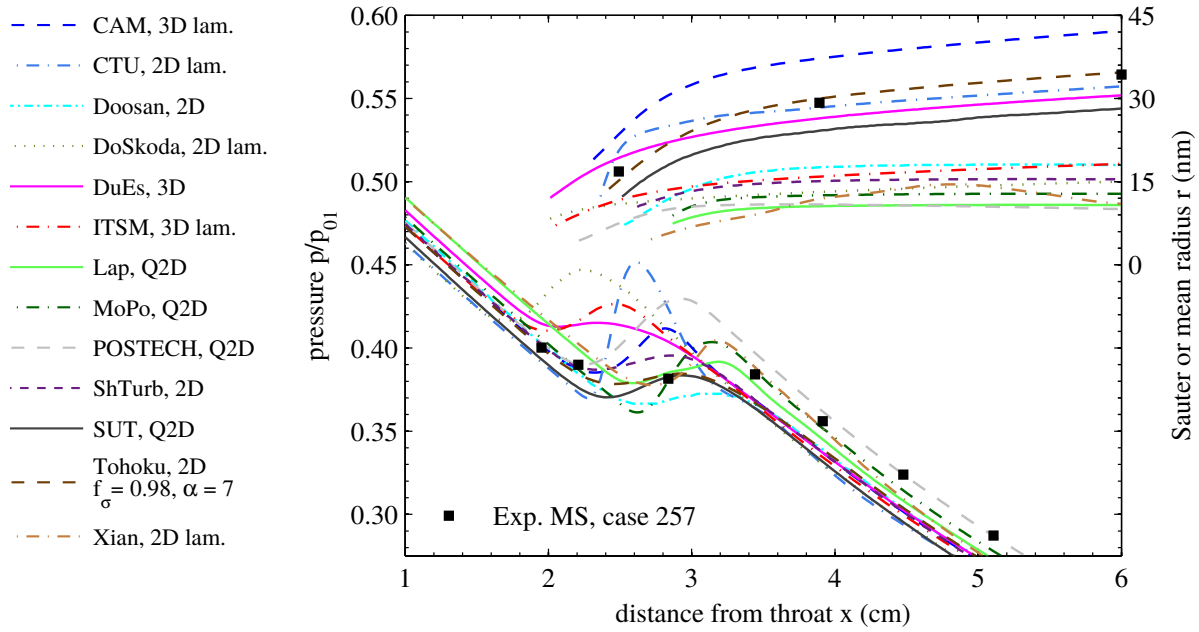

Fig. 5: Moses and Stein nozzle, case 257, $p_{01} = 67.66\,\mathrm{kPa}$ and $T_{01} = 376.7\,\mathrm{K}$

predicts condensation upstream of the experiment, whereas the SUT model obtains the same good agreement as for the lower pressure case. Lap and ShTurb (both of whom predicted the Wilson pressure too far downstream for the previous case) now obtain much closer agreement with measured pressures using the same settings, but droplet radii are still under-predicted. The same applies to the results of Xian, but in addition the droplet radius shows curious behaviour in the rear part or the nozzle.

From Fig. 5 it is seen that models which give reasonable agreement with measured upstream pressures tend to under-predict the pressure in the downstream section. In order to shed some light on this, boundary layer profiles predicted by a few of the methods using the medium mesh (for which even laminar profiles are resolved by at least 18 grid points) are shown in Fig. 6. It is clear that the choice of turbulence model (and probably its implementation) cause significant differences in the boundary layer growth. The calculation of MoPo has the largest boundary layer thickness yielding results that agree well with downstream pressure measurements, but even this fast-growing turbulent boundary layer cannot fully resolve the discrepancies. On the other hand, there is no clear evidence for any other form of blockage. The POSTECH results give the best agreement in the far downstream region but, given that this method tends to over-predict exit pressures for all the other cases, this agreement may be coincidental. In any case, the differences are not due to the turbulence modelling since POSTECH is using the Spalart-Allmaras (SA) model which (although not shown in the figure) gives a very similar boundary layer to that of CAM when using the SA model.

For the Moses and Stein test 257 with the higher Wilson pressure the majority of methods predict condensation too far upstream. This suggests the possibility that either the computed nucleation rate or droplet growth rate are too high. To investigate this further some additional calculations were undertaken using the CAM model with various adjustments to nucleation and growth modelling. These calculations have been carried out in 2D (i.e., not accounting for boundary layer growth on the plane side-walls) and assuming a turbulent flow because, as a 3D laminar model, this gives a good agreement for the pressure distribution upstream of condensation but also improves the shape of the condensation pressure rise. (Starzmann et al. (2016) showed that the displacement thickness of a turbulent boundary layer is less influenced by condensation heat release than a laminar boundary layer which damp the pressure rise.)

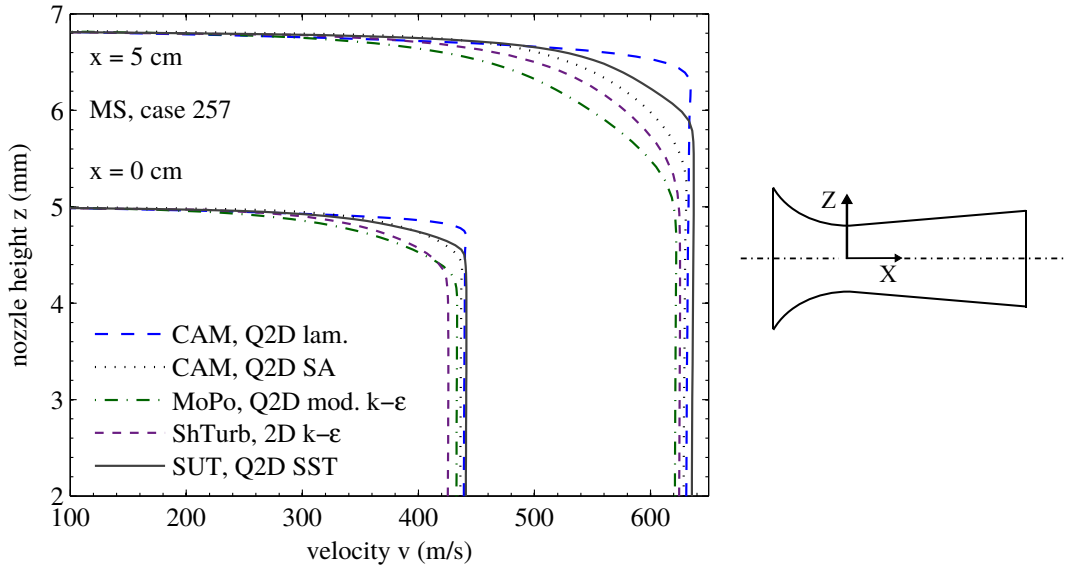

Fig. 6: Boundary layers for the Moses and Stein nozzle, case 257

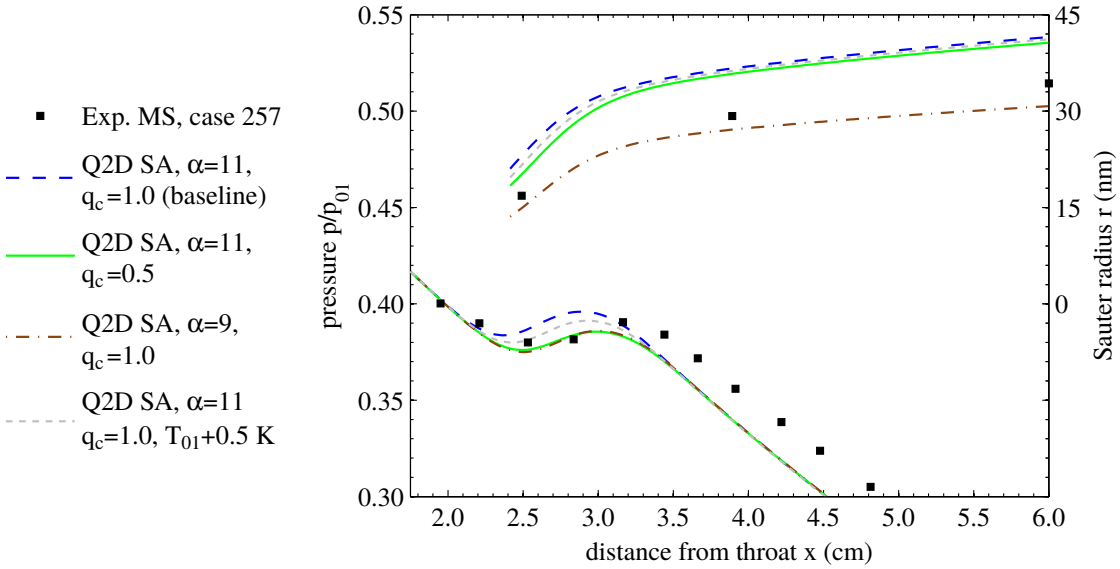

Fig. 7: Parameter variation using model CAM for the Moses and Stein nozzle, case 257

Although a 2D turbulent calculation is clearly not realistic, it provides a common basis for comparing modifications to nucleation and growth modelling.

With default settings (the baseline case in Fig. 7) the Wilson point is too far upstream and the droplet size is over-predicted. Young (1982) originally suggested that the condensation coefficient q_c might be pressure dependent. However White and Young (1993) later proposed varying instead α in Young's growth model with pressure since the consensus view is that q_c should be unity. (Note that α controls the ratio between the condensation and evaporation coefficients which are arguably different under non-equilibrium conditions.) Results with various combinations of q_c and α are shown in Fig. 7. Young (1982) found that for test 257 a q_c value of 0.2 gives best agreement with the measurements but for the present computations a value of 0.5 is needed. In summary, from these results it may be concluded that reducing α from its baseline value and retaining $q_c = 1$ is probably the best strategy because this reduces the calculated Wilson pressure and simultaneously the droplet radius. However, it has to be remembered that

the uncertainty of the measured droplet size data is perhaps ±20% which makes a proper validation quite precarious.

Another possibility why for test 257 the condensation is predicted too far upstream is the uncertainty in the recorded stagnation temperature which, according to Moses and Stein (1978) is roughly 0.5 K. In Fig. 7 a computation with baseline settings but T_{01} increased by 0.5 K reveals that this change is not sufficient to align predictions with experiment.

Nonetheless, the picture may well change with a more successful means of modelling boundary layer blockage, such as 3D calculations with correct transition modelling. In this respect, it should be mentioned that Young (1982) used a 1D method with the effective area inferred from the dry pressure distribution which is certainly the most preferable way to validate wet-steam models.

6 Constant expansion rate nozzle

Both nozzles considered so far have their drawbacks: the Moore nozzle due to its strong 2D effects and the Moses and Stein nozzle due to its narrow throat and consequent sensitivity to boundary layer blockage. For this reason, a new geometry (the "Mystery" nozzle) was designed using the method described by Gyarmathy and Meyer (1965). The intention is to provide an essentially 1D flow, free from expansion and compression waves, and with an approximately constant (dry flow) expansion rate in the anticipated condensation zone. Gyarmathy and Meyer's method is based on 1D (dry) perfect gas conservation equations and requires the stagnation enthalpy, the desired expansion rate and the effective isentropic expansion factor γ as inputs. The original paper is in German, but the method is also described in English by Starzmann et al. (2016). The Mystery nozzle was designed with a throat height of 40 mm and an expansion rate of $3500\,s^{-1}$ (representative of an LP turbine), based on $c_p = 1900\,\mathrm{J\,kg^{-1}\,K^{-1}}$, $\gamma = 1.32$ and $T_{01} = 100°\mathrm{C}$. The inlet section is defined by a simple parabolic curve. The Mystery nozzle is intended to mitigate the uncertainties associated with viscous modelling, but its obvious disadvantage is the lack of experimental data. Participants of the project were asked to consider only two-dimensional flow (since this is solely a numerical comparison) that is fully turbulent with zero inlet turbulence intensity. Calculations were requested for two inlet temperatures.

6.1 Mystery nozzle with high inlet temperature

For the first case the inlet stagnation conditions are $p_{01} = 110\,\mathrm{kPa}$ and $T_{01} = 417\,\mathrm{K}$, leading to a Wilson point pressure of about 30 kPa. Results are shown in Fig. 8 and indicate similar trends to the Moses and Stein cases. The scatter is quite significant (though it should be borne in mind that the figure focuses on a small section of the nozzle) and there is a surprising variation in the shape of the condensation-induced pressure changes, with two methods predicting undulations in the downstream region. Furthermore, there is modest variation in the predicted pressure distribution upstream of condensation (but downstream of the throat) and in retrospect it may have been wise to request inviscid calculations or to specify a even bigger nozzle throat height. The scatter for the predicted droplet size is also significant with radii ranging from 14 nm (Lap) to 86 nm (CAM), although the latter would be reduced by the use of a lower value of α (Wilson pressure dependency) in line with the comments of Sec. 5.2 and the findings of White and Young (1993).

6.2 Mystery nozzle with lower inlet temperature

The second case is at the same stagnation pressure but T_{01} is reduced to 388 K, thereby increasing the Wilson pressure to about 50 kPa. Fig. 9 shows that the spread of results is even more dramatic. This is mainly due to the fact that some of the methods (especially those that have a tendency to predict condensation early) are clearly predicting supercritical heat addition with an embedded shockwave. As already noted, the participants use a variety of nucleation and growth models and parameters as well as different equations of state. Nonetheless, the very

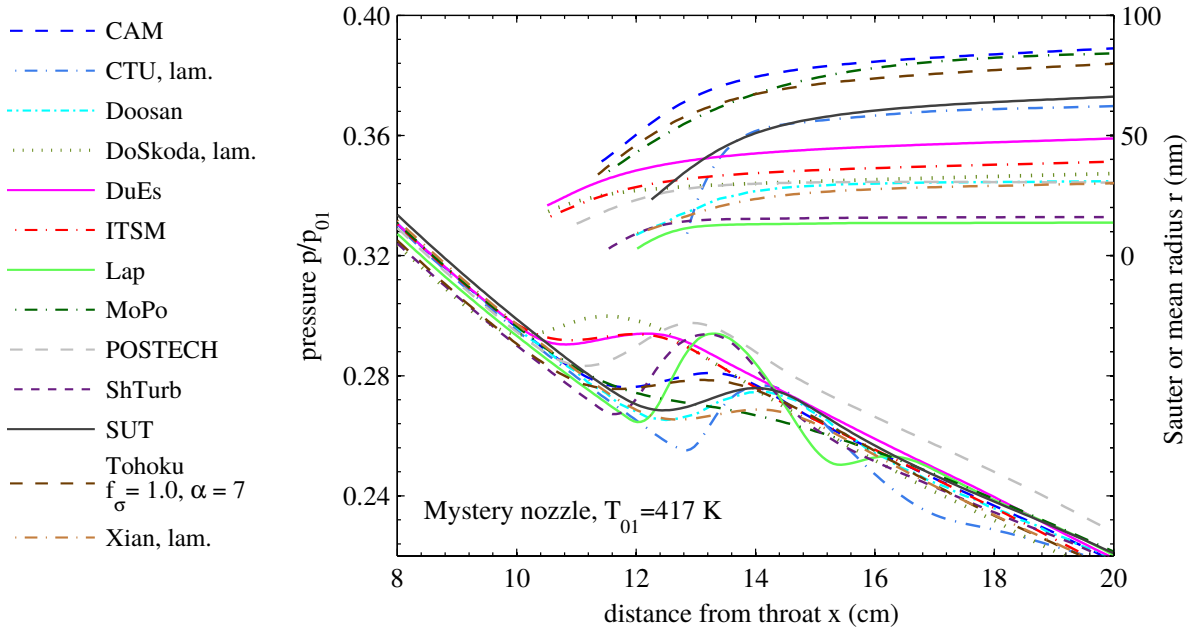

Fig. 8: Pressure and droplet radius for the Mystery nozzle, $p_{01} = 110\,\mathrm{kPa}$ and $T_{01} = 417\,\mathrm{K}$

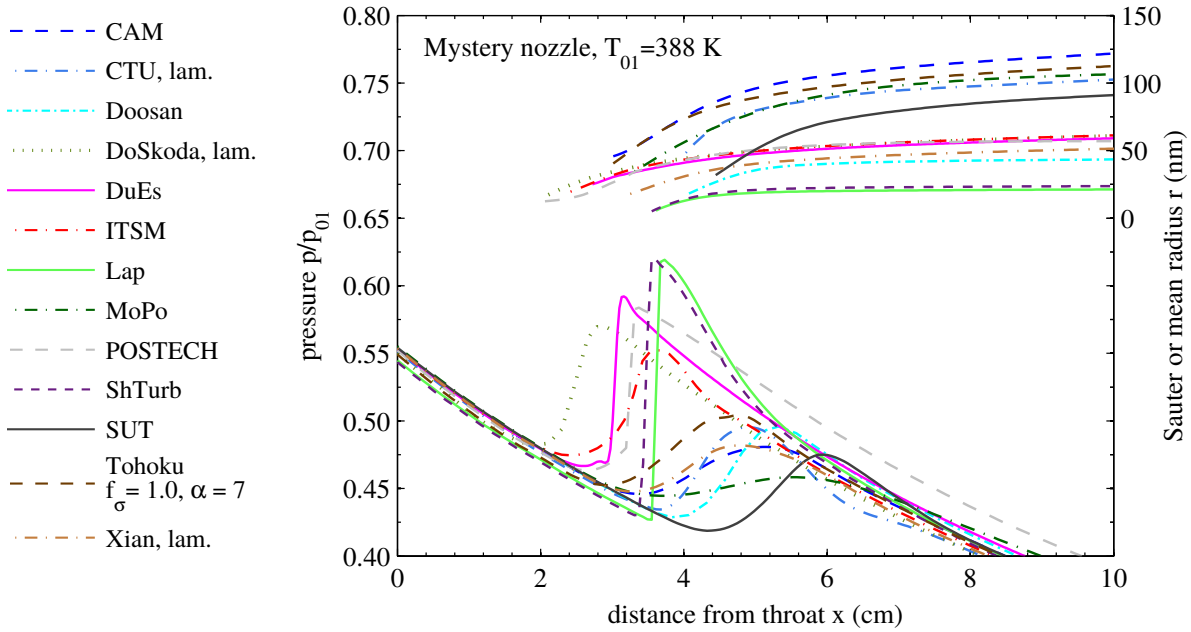

Fig. 9: Pressure and droplet radius for the Mystery nozzle, $p_{01} = 110\,\mathrm{kPa}$ and $T_{01} = 388\,\mathrm{K}$

substantial diversity in these results is striking and it may well be that differences in the way the models are implemented and the underlying numerical methods are contributing factors.

7 The impact of various model parameters and assumptions

The vast range of modelling approaches, numerical methods and parameter settings means that it is very difficult to deduce major trends by comparing results from all participants. The effect of varying some of the key parameters and assumptions is therefore examined in this section, with variations restricted to implementations within a single solver where possible, or otherwise to solvers with other features in common.

Table 1: Reynolds numbers at the throat for different nozzles

Nozzle test	Inlet pressure p_{01} (kPa)	Reynolds number $\mathrm{Re}_{x,\mathrm{throat}}$
Moore B	25.0	4.1×10^5
Moses and Stein (252)	40.5	3.1×10^5
Moses and Stein (257)	67.7	5.1×10^5
Mystery ($T_{01} = 388\,\mathrm{K}$)	110.0	2.4×10^6
Mystery ($T_{01} = 417\,\mathrm{K}$)	110.0	2.0×10^6

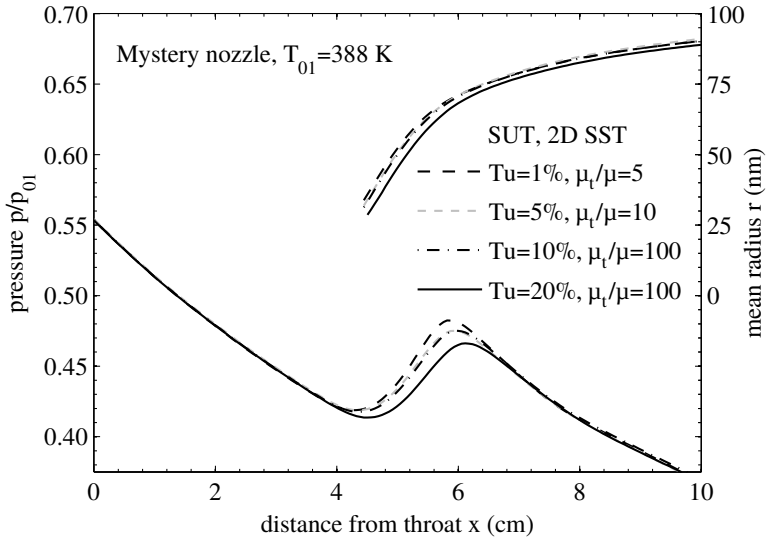

Fig. 10: Influence of inlet turbulence for the Mystery nozzle

7.1 Influence of inlet turbulence intensity

The Reynolds numbers Re_x based on the axial coordinate at the throat are summarised for the different nozzles in Table 1. Except for the Mystery nozzle (for which the larger dimensions and the higher pressure result in higher Re_x) they are all in the transition region. Given the impact of compressibility effects and the strongly favourable pressure gradients, it is not clear what the state of the boundary layers will be. A study conducted by Starzmann et al. (2016) concluded that the experimental data were consistent with transition occurring downstream of the throat for both the Moore et al. and Moses and Stein nozzles. Furthermore, the condensation pressure rise may well be instrumental in triggering transition, though there are currently no experimental data nor numerical studies to confirm this.

In addition to the state of the boundary layers, the level of free-stream turbulence is also unknown. However, the SUT team undertook calculations for the Mystery nozzle with different inlet turbulence intensities Tu in order to examine its influence. They also varied the eddy viscosity ratio μ_t/μ. Their results are presented in Fig. 10 and show that, provided the turbulent intensity is kept within a reasonable range, neither the pressure distribution nor droplet size are significantly affected. This finding is in keeping with the single test conducted by Moore et al. (1973) with a turbulence grid installed at the nozzle inlet, but it is worth noting that the direct impact of turbulence on neither transition nor nucleation are modelled in the calculations.

7.2 Droplet size distribution modelling

As described in White (2000) or Hughes et al. (2015) there are several different ways of representing the droplet size distribution within a given numerical approach. Of these, the discrete spectrum method (which is most easily implemented in a Lagrangian framework) is deemed the most accurate whereas the monodispersed method (which may be incorporated into either

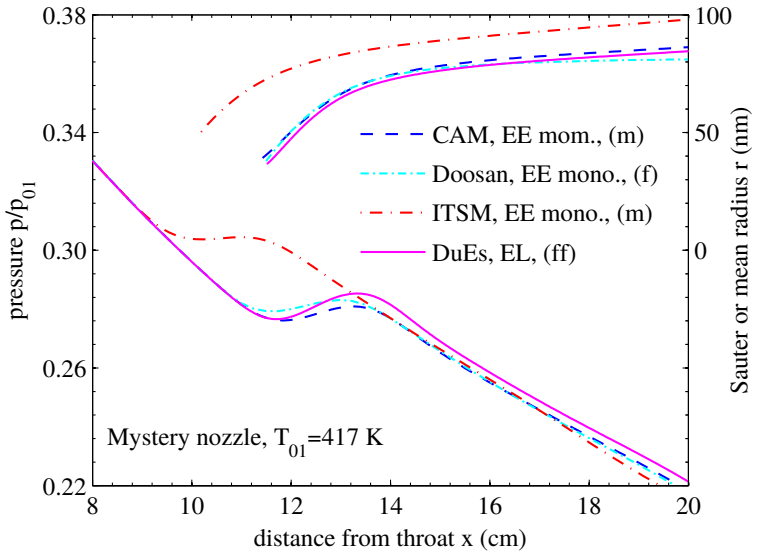

Fig. 11: Influence of various droplet representation methods for the Mystery nozzle

fully Eulerian or mixed Eulerian-Lagrangian methods) is the simplest and least computationally intensive. Intermediate between these are the various moment-based methods. Further explanations and a comparison between these methods are given in the paper by Hughes et al. (2015).

All three methods have been used within this project and results are compared for the Mystery nozzle in Fig. 11. Although these results have been obtained with different solvers, for the present study they all use the same equation of state (IAPWS-IF97), the same formulas for supplementary properties, and the same nucleation and growth models with the same growth parameters ($\alpha = 11$ and $\beta = 0$). The three size-modelling approaches yield similar results, which is not surprising since simple (sub-critical) condensation within nozzles tends to produce droplets with a very narrow range of sizes. However, the ITSM result is not in keeping with the other methods and this is of particular interest because ITSM is using a common monodispersed wet-steam model implemented within the commercial Ansys CFX solver. Various studies of the ITSM group (see Grübel et al., 2015; Starzmann, 2015) showed that in order to match this model with experimental data a significant adjustment to the nucleation model is needed (e.g. an increase of planar surface tension of about 10%). Note that the Eulerian-Lagrangian method of DuEs is also based on Ansys CFX but does not suffer from the same premature condensation problem.

Differences between the CAM, Doosan and DuEs methods are quite minor and do not merit further discussion but, in passing, it is worth noting that, at least for the Mystery nozzle, the DuEs method exhibited the greatest level of grid dependence. Whereas most methods converged to a grid-independent solution with either the medium (m) or fine (f) grids, the DuEs method required a very fine (ff) grid. (Droplet sizes increased by 7% between the (m) and (f) grids, and by a further 4% between the (f) and (ff) grids.) This result is surprising because mixed Eulerian-Lagrangian methods should in principle require less dense grids than the fully Eulerian methods.

7.3 Sensitivity to nucleation rate modelling

All participants modelled droplet formation by means of the classical nucleation theory. This theory and especially its application to wet-steam flows has been reviewed by Bakhtar et al. (2005). A derivation of the theory and discussion of the various corrections is too lengthy to reproduce here and so only the final nucleation expressions are cited. However, the influence of the various adjustments to the classical expression adopted by the project participants is considered in detail.

The classical homogeneous nucleation rate per unit volume of mixture is

$$J_{\mathrm{CL}} = q_{\mathrm{c}} \, \frac{\varrho_{\mathrm{g}}^2}{\varrho_{\mathrm{f}}} \sqrt{\frac{2\sigma_{\mathrm{g}}}{\pi m_{\mathrm{m}}^3}} \exp\left(-\frac{4\pi\sigma_{\mathrm{g}}}{3\,\mathrm{k_B} T_{\mathrm{g}}} r_{\mathrm{crit}}^2 \right) \quad , \tag{1}$$

where q_{c} is the condensation coefficient, σ_{g} the planar surface tension, m_{m} the mass of a water molecule, $\mathrm{k_B}$ is Boltzmann's constant, T_{g} the temperature of the vapour, ϱ are the densities and the subscripts 'g' and 'f' denote to the vapour phase and saturated liquid respectively. The Kelvin-Helmholtz critical radius is given by,

$$r_{\mathrm{crit}} = \frac{2\sigma_{\mathrm{g}}}{\varrho_{\mathrm{f}} \mathrm{R} T_{\mathrm{g}} \ln(S)} \quad , \tag{2}$$

where $S = p/p_{\mathrm{s}}$ is the supersaturation ratio. The critical radius may also be written in terms of subcooling and latent heat h_{fg} by incorporating the Clausius-Clapeyron relation into eq. (2), giving

$$r_{\mathrm{crit}} = \frac{2\sigma_{\mathrm{g}} T_{\mathrm{s}}}{\varrho_{\mathrm{f}} h_{\mathrm{fg}} \Delta T} \quad . \tag{3}$$

None of the participants used Courtney's (1961) correction (which reduces J_{CL} by a factor of S) but many applied the non-isothermal correction of Kantrowitz (1951). This accounts for the fact that the embryonic liquid clusters are generally hotter than the surrounding vapour (since latent heat must be released) and typically reduces nucleation by two orders of magnitude. Kantrowitz's correction takes the form

$$J_{\mathrm{CL,NISO}} = \frac{J_{\mathrm{CL}}}{1+\phi} \tag{4}$$

where

$$\phi = 2\frac{\gamma-1}{\gamma+1} \frac{h_{\mathrm{fg}}}{\mathrm{R} T_{\mathrm{g}}} \left(\frac{h_{\mathrm{fg}}}{\mathrm{R} T_{\mathrm{g}}} - \frac{1}{2} \right) \quad . \tag{5}$$

The two other main adjustments to classical theory adopted by the various project participants were (i) variation of the condensation coefficient q_{c} (the standard value for which is unity) and (ii) variation of the surface tension σ. For a planar interface, σ is only a function of temperature and although different formulas have been adopted for $\sigma(T)$ the greatest discrepancy over the temperature range of interest is only 1.5% (see Fig. 13). By contrast, the extent to which surface tension depends on cluster size remains an unresolved issue (see for example Wegener, 1969; Bakhtar et al., 2005). Most participants have used flat-film values for σ but POSTECH uses a Tolman length approach according to Onischuk et al. (2006) whereas DuEs and Tohoku simply multiply the planar surface tension by a factor f_σ. (Tohoku varies f_σ between 0.92 and 1.0 for the different nozzle cases, but DuEs uses a constant value of $f_\sigma = 0.95$.)

Fig. 12 shows the effect of the above adjustments on nucleation rates over a range of subcooling values and at a pressure of 50 kPa. At a typical Wilson point subcooling of 30 K the non-isothermal correction is seen to have a significant effect, but this is more or less cancelled out by a 5% reduction in σ. The impact of q_c is relatively minor (J simply scales with q_c), especially given that a value of 0.1 is probably unrealistically low.

Fig. 14 shows the impact of the above-described modifications on the pressure distributions and droplet sizes within the Mystery and Moses and Stein nozzles. All calculations were undertaken using the CAM method, employing Young's droplet growth model with $\alpha = 11$ and $\beta = 0$. The fractional change in Wilson point pressure brought about by the various changes in the nucleation expression are similar for the two nozzles, though the faster expansion for the Moses and Stein case of course means that the axial shift (in terms of cm) is smaller. The non-isothermal correction significantly delays the pressure rise and since fewer droplets are formed the droplet

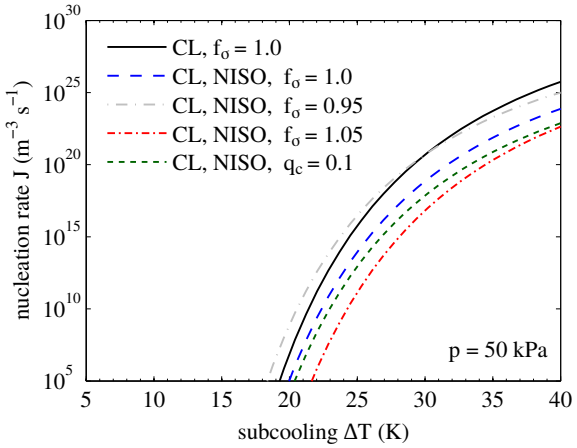

Fig. 12: Nucleation rate at constant pressure

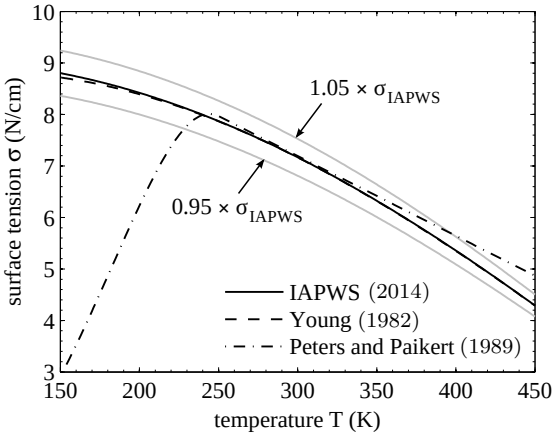

Fig. 13: Planar surface tension for water

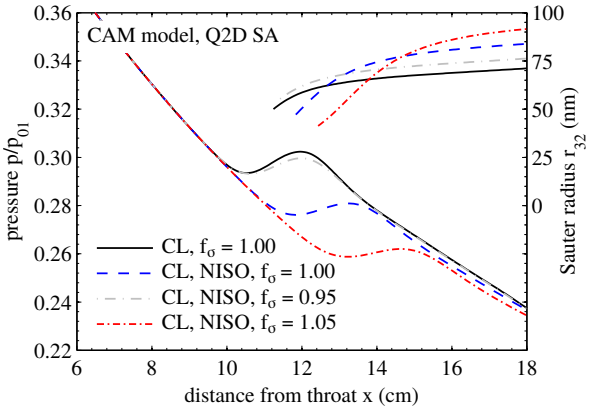

a) Mystery nozzle with $T_{01} = 417\,\mathrm{K}$

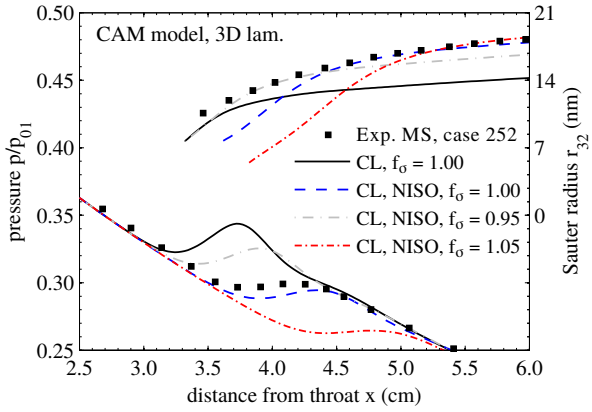

b) Moses and Stein nozzle, case 252

Fig. 14: Influence of surface tension and non-isothermal correction on nozzle flows

size is increased. These effects are approximately cancelled out by 5% reduction in σ for the Mystery nozzle, but not for the Moses and Stein case. This is because the higher expansion rate in the latter case results in a Wilson point subcooling of 40 K (versus 32 K for the Mystery nozzle) at which the recovery in nucleation rate by the reduction in σ is less, as seen in Fig. 12.

In general, nucleation rates need to be reduced relative to the original classical expression in order to match theory and experiment. This could be achieved by either an increase in σ or by Kantrowitz's correction, but the latter probably has a more sound physical basis. Other possible corrections to the theory are discussed in Bakhtar et al. (2005).

7.4 Sensitivity to droplet growth modelling

A comprehensive overview of various droplet growth models was given by Young (1982) and a more recent review provided Lamanna (2000). The three main growth expressions used by the project participants are those due to Gyarmathy (1962), Young (1982) and Hill (1966). A brief account of each of these is given below.

1. *Gyarmathy's growth law.* This was one of the first commonly-adopted models and is hereinafter referred to as 'Gy62'. Gyarmathy's growth law essentially entails solving the droplet energy equation alone on the basis that growth is limited by the rate at which latent heat is transferred back to the vapour. The original expression is

$$\frac{\mathrm{d}r}{\mathrm{d}t} = \frac{h}{\varrho_\mathrm{f} h_\mathrm{fg}}(T_\mathrm{l} - T_\mathrm{g}) = \frac{\lambda_\mathrm{g}\,(T_\mathrm{l} - T_\mathrm{g})}{\varrho_\mathrm{f} h_\mathrm{fg} r\,(1 + 3.18\mathrm{Kn})} \quad , \tag{6}$$

where the heat transfer coefficient h depends on the Knudsen number $\mathrm{Kn} = \bar{l}/(2r)$, accounting for the fact that growing droplets span sizes from smaller than to greater than the mean free path length $\bar{l}$ [1]. Gyarmathy showed that the droplet temperature T_l rapidly adopts a quasi-steady value which may be approximated by

$$T_\mathrm{l} - T_\mathrm{g} = \Delta T \left(1 - \frac{r_\mathrm{crit}}{r}\right) \quad , \tag{7}$$

where the subcooling ΔT is the vapour subcooling. This algebraic relation makes droplet growth modelling much easier as it eliminates the need to solve simultaneous heat and mass balances for the droplet.

2. *Young's growth law.* By comparing 1D calculations with experiments for many test cases Young (1982) showed that adjustments were needed to Gyarmathy's growth rate to "ensure optimum agreement" with measurements. He proposed a modification to eq. (7) based on careful consideration of Gyarmathy's assumptions. A detailed derivation is given by Young (1982), but the final growth expression (henceforth referred to as 'Yg82') is

$$\frac{\mathrm{d}r}{\mathrm{d}t} = \frac{\lambda_\mathrm{g}\,(1 - r_\mathrm{crit}/r)\,\Delta T}{\varrho_\mathrm{f} h_\mathrm{fg} r \left(\dfrac{1}{1+2\beta\mathrm{Kn}} + 3.78(1-\nu)\dfrac{\mathrm{Kn}}{\mathrm{Pr}}\right)} \tag{8}$$

where Pr is the Prandtl number and

$$\nu = \frac{\mathrm{R}T_\mathrm{s}}{h_\mathrm{fg}} \left(\alpha - 0.5 - \frac{2-q_\mathrm{c}}{2q_\mathrm{c}} \left(\frac{\gamma+1}{2\gamma}\right) \left(\frac{c_{pg} T_\mathrm{s}}{h_\mathrm{fg}}\right)\right) \quad . \tag{9}$$

Young's model contains two modelling parameters, namely β in eq. (8) and α in eq. (9). The first relates to the Langmuir model in which free-molecular processes are assumed to occur in the region immediately surrounding the droplet and continuum processes occur further away, the interface between the two zones being located at $r + \beta\bar{l}$. Most participants using Yg82 set $\beta = 0$ but a few followed Guha and Young (1991) for which $\beta = 2$. The growth parameter α was introduced to express the relationship between the condensation and evaporation coefficients (q_c and q_e) in terms of a Taylor expansion. Young found that $\alpha = 9$ was a suitable value, but the best choice is likely to depend on other aspects of wet-steam modelling such as the equation of state. Various values have been used by the different participants, and others have specified a constant value of the quantity ν.

3. *Hill's growth law.* Hill (1966) proposed a growth law based on the solution of the energy equation in the free molecular regime. It is therefore only strictly valid for large Knudsen numbers (i.e., small droplets) and takes the form

$$\frac{\mathrm{d}r}{\mathrm{d}t} = \frac{p}{\varrho_\mathrm{f} h_\mathrm{fg} \sqrt{2\pi \mathrm{R} T_\mathrm{g}}} \frac{\gamma+1}{2\gamma} c_{pg}\,(T_\mathrm{s} - T_\mathrm{g}) \quad . \tag{10}$$

Hill's growth rate (henceforth 'Hi66') is independent of droplet size and in passing it is worth noting that this implies that the moment method (originally developed for condensing flow by Hill) is exact when used in conjunction with this model.

Fig. 15a compares the different droplet growth models for a modest subcooling of $\Delta T = 15°\mathrm{C}$. The effects of common choices for α and β are also shown. The variation of the modelling parameter α over the wide range 0 to 11 may at first seem rather unsatisfactory, but Fig. 15a shows that in fact a value of around 4 corresponds to Gyarmathy's growth law whereas $\alpha = 11$ only doubles the peak growth relative to Gy62. Fig. 15b shows the correspondence between α and ν for reference purposes (for example $\nu = 0.2$ specified by ShTurb corresponds to $\alpha \approx 4$ whereas $\nu = 0.9$ assumed by CTU equates to $\alpha \approx 14$).

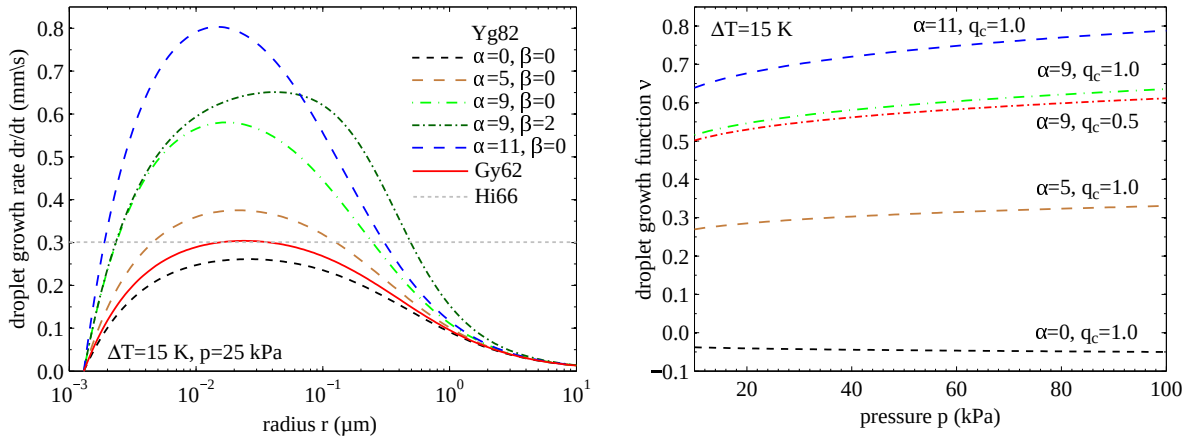

a) Growth rates for different models **b)** Influence of parameter α on growth function ν

Fig. 15: Influence of various models and parameters on the droplet growth rate

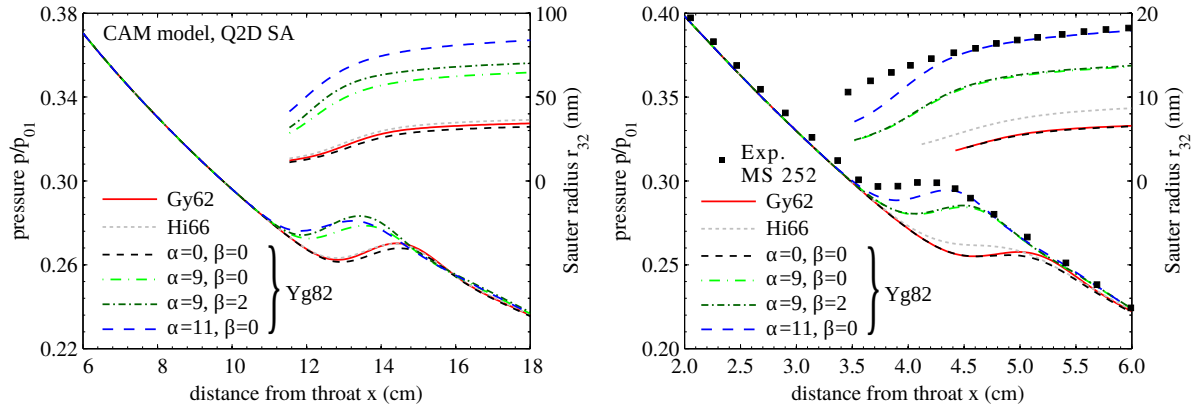

a) Mystery nozzle with $T_{01} = 417\,\mathrm{K}$ **b)** Moses and Stein nozzle, case 252

Fig. 16: Example calculations for different droplet growth models using the CAM model

Fig. 16 compares the effect of different growth models and modelling parameters on the pressure distribution and droplet sizes for the Mystery and Moses and Stein nozzles. Calculations were undertaken using classical nucleation theory with Kantrowitz's correction. The growth models of Hill and Gyarmathy and Young's model with $\alpha = 0$ all result in a late prediction of the condensation pressure rise, reflecting the relatively slow growth rate. For the Mystery nozzle predicted droplet sizes for the models Gy62, Hi66 and Yg82 (with $\alpha = 0$) are between 10 and 30 nm and in this regime their growth rates do not differ significantly. The results for these growth laws are consequently very similar. Larger differences are apparent for the Moses and Stein nozzle because the higher expansion rate produces smaller droplets for which the various growth laws differ. By contrast, the influence of β is only significant for the larger droplets in the Mystery nozzle.

As discussed earlier, best agreement with experimental data is obtained with $\alpha = 11$ (at least when using the CAM method) for the lowest pressure tests (Moore nozzle B and Moses and Stein test 252) but there is evidence to suggest that lower values of α are required at higher pressures. More experimental data are however required to draw any firm conclusions.

[1]Gyarmathy uses the standard expression for mean free path $\bar{l} = 1.5\mu_g\sqrt{RT_g}/p$, whereas Ansys CFX replaces the factor 1.5 by 1.88. ITSM and DuEs have however both used the standard expression.

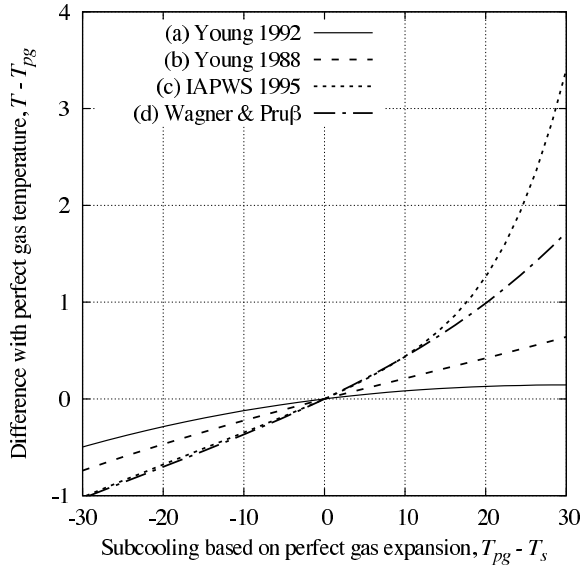

Fig. 17: Differences between equations of state, taken from White and Senoo (2016)

7.5 Sensitivity to the equation of state

Most groups modelling wet-steam are now using the industrial formulation IAPWS-IF97 (2007) for the equation of state, or at least an approximation thereof. Young's (1988) virial gas equation is also common and has been applied by Lap, ShTurb and Xian. CTU, DoSkoda, POSTECH and Tohoku, however, use only a simple equation of state based on perfect gas relations.

The influence of different equations of state has not been extensively studied so far in the context of wet-steam flow, but it is indeed a further source of uncertainty. To highlight this fact, Fig. 17 shows differences in temperatures computed with various equations of state[2] during an isentropic expansion. (The ordinate and the abscissa are related to the temperature for perfect gas flow, with a common datum at the saturated condition.) At typical Wilson point conditions the curves show differences of around 1 to 2 K which are quite significant in the context of nucleating flow. It is worth recalling that no experimental data are available for subcooled vapour and so none of the equations are properly validated in this region.

Results using some of the different equations of state are shown in Fig. 18, once again for the Mystery and Moses and Stein nozzles. These calculations were undertaken using the CAM method with nucleation, growth and other modelling as detailed in Tab. A2. Firstly it is notable that upstream of the condensation zone the different equations yield only very minor differences in pressure distribution, so the different equations cannot practicably be "validated" by comparison of dry-expansion pressures with measurement. The discrepancy in predicted Wilson points is however very clear, stemming from the temperature differences shown in Fig. 17. The observed shifts in condensation zone obviously add to the uncertainty and difficulty in validating condensing flow theory.

8 Conclusions

The main purpose of this project has been to review and investigate the reliability of numerical models for condensing steam flows. Calculations have been undertaken for several nozzles by the thirteen participating groups, using a range of wet-steam flow solvers. Some of the methods

[2]The figure includes the virial equation of Young (1988); an equation of the form $p = \varrho_g R T_g (1 + Z)$ where $Z(p,T_g)$ is a compressibility parameter (see Young, 1992) and the IAPWS-95 (2014) scientific formulation. The so-called Gas-equations of Wagner and Pruß (2002) contain corrections to the IAPWS-95 formulation to model the subcooled region. The results are almost identical to IAPWS-IF97 because the latter one was developed based on the IAPWS-95 formulation and the Gas-equations.

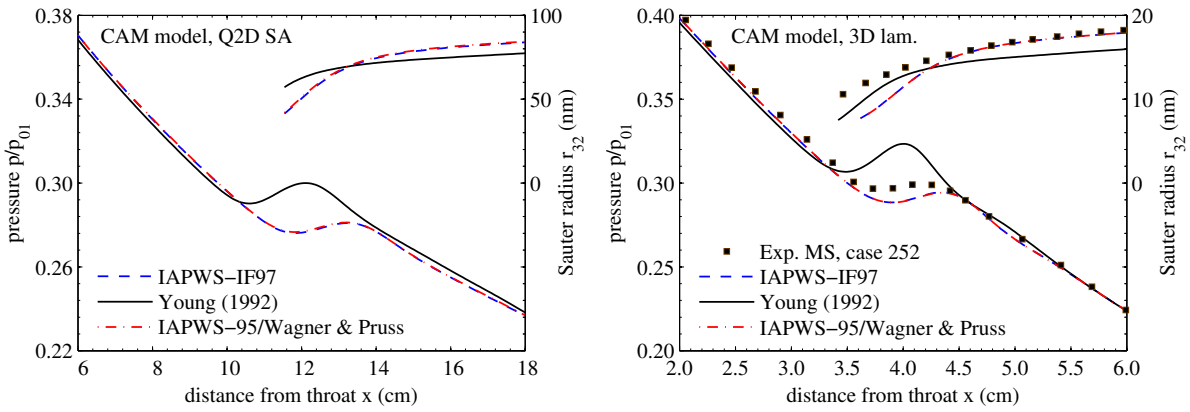

a) Mystery nozzle with $T_{01} = 417\,\mathrm{K}$ **b)** Moses and Stein nozzle, case 252

Fig. 18: Influence of the equation of state on condensing nozzle flows

achieve reasonable agreement with experimental data but the variability of the results is quite striking. Much of this variability stems from differences in the adopted condensation models, but it would seem that some of it also arises from how these models are implemented and the underlying flow solvers within which they are incorporated. Given the diversity of the various methods it is difficult to draw firm conclusions, but the following comments are nonetheless appropriate:

1. Uncertainties in nucleation theory, droplet growth *and* the equation of state all contribute to the difficulty in validating condensing flow theory. Given the complex interaction between these it is not surprising that no general consensus has emerged as to the best combination of models and modelling parameters.

2. The above uncertainties are compounded by unknown aspects of the nozzle boundary layers, notably their state (laminar or turbulent) and the effective blockage caused by them. In this respect, attention has been drawn to deficiencies in the tested nozzle designs, even though these nozzles rank amongst the best in terms of the measured data available.

3. Despite the above difficulties, it can be confirmed that nucleation rates need to be reduced relative to classical theory (e.g., by the non-isothermal correction) and droplet growth rates increased relative to Gyarmathy's growth law (e.g., by Young's model and associated growth parameter α) in order to achieve agreement with experiment for a range of test cases.

4. In order to separate out boundary layer blockage effects from the uncertainties of condensation modelling it would seem wise to resort to the old-fashioned method of using dry-expansion pressure measurements to infer the effective nozzle area variation (i.e., including the effects of blockage) and then to undertake one-dimensional, inviscid calculations.

5. Finally, a well-worn statement needs to be repeated, namely that the experimental data base is not sufficient to achieve proper validation. Experiments need to be conducted over a broader range of conditions, but attention also needs to be given to the design of nozzles to avoid undesirable 2D effects, and sensitivity to boundary layer blockage. Such experiments should follow carefully the guidelines written by Gyarmathy (1976, p. 137 ff) forty years ago.

Authors' contributions

The first author led and managed the project, coordinated the contributions from the participants, undertook the majority of the analysis of the results and drafted the manuscript. The

second and third authors contributed to drafting the manuscript and advised on its content. The remaining authors are the project contributors and some of whom made suggestions for the paper content.

Acknowledgement

The lead authors would like to acknowledge all the colleagues who have participated in this international collaboration. They are also thankful to EPSRC for funding this research as a part of the "Future Conventional Power Consortium".

References

Avetissian, A. R.; Philippov, G. A.; Zaichik, L. I.: The effect of turbulence on spontaneously condensing wet steam flow, *Nuclear Engineering and Design*, 235:1215–1223, 2005

Bakhtar, F.: Special Issue on Wet Steam - Part 1, *Proc. Inst. Mech. Eng. C, J. Mech. Eng. Sci.*, 218(8), 2004

Bakhtar, F.: Special Issue on Wet Steam - Part 2, *Proc. Inst. Mech. Eng. C, J. Mech. Eng. Sci.*, 219(12), 2005

Bakhtar, F.; Young, J. B.; White, A. J.; Simpson, D. A.: Classical nucleation theory and its application to condensing steam flow calculations, *Proc. Inst. Mech. Eng. C, J. Mech. Eng. Sci.*, 219(12):1315–1333, 2005

Barschdorff, D.: Verlauf der Zustandsgrößen und gasdynamische Zusammenhänge bei der spontanen Kondensation reinen Wasserdampfes in Lavaldüsen, *Forsch. Ingenieurwes.*, 37(5):146–157, 1971

Chandler, K. D.; White, A. J.; Young, J. B.: Non-equilibrium wet-steam calculations of unsteady low-pressure turbine flows, *Proc. IMechE, Part A: J. Power and Energy*, 228(2):143–152, 2014

Courtney, W. G.: Remarks on Homogeneous Nucleation, *J. Chem. Phys.*, 35(6):2249–2250, 1961

Eckert, E. R. G.; Drake, R. M.: *Analysis of Heat and Mass Transfer*, McGraw Hill Co., 1972

Grübel, M.; Starzmann, J. Schatz M.; Eberle, T.; Vogt, D. M.; Sieverding, F.: Two-Phase Flow Modeling and Measurements in Low-Pressure Turbines: Part 1 – Numerical Validation of Wet Steam Models and Turbine Modeling, *Trans. ASME, J. Eng. Gas Turb. Power*, 137(4), 2015

Guha, A.; Young, J. B.: Time-marching prediction of unsteady condensation phenomena due to supercritical heat addition, in: *Turbomachinery: Latest Developments in a Changing Scene*, Proc. Instn. Mech. Eng., pp. 167–177, Paper C423/057, 1991

Gyarmathy, G.: *Grundlagen einer Theorie der Naßdampfturbine*, Dissertation, ETH Zürich, 1962

Gyarmathy, G.: Condensation in Flowing Steam, in: *Two Phase Steam Flow in Turbines and Separators*, Hemisphere Publishing Corporation, ISBN 0-07-042992-8, 1976

Gyarmathy, G.; Meyer, H.: *Spontane Kondensation Teil 2: Einfluss der Entspannungsschnelligkeit auf die Nebelbildung in übersättigtem Dampf*, VDI-Forschungsheft 508, VDI Verlag GmbH, (in German), 1965

Halama, J.; Benkhaldoun, F.; Fořt, J.: Flux schemes based finite volume method for internal transonic flow with condensation, *Int. J. Numer. Meth. Fluids*, 65(8):953–968, 2010a

Halama, J.; Benkhaldoun, F.; Fořt, J.: Numerical modeling of two-phase transonic flow, *Math. and Computers in Simulation*, 80(8):1624–1635, 2010b

Halama, J.; Fořt, J.: Numerical simulation of transonic flow of wet steam in nozzles and turbines, *Computing*, 95(1):303–318, 2013

Heiler, M.: *Instationäre Phänomene in homogen/heterogen kondensierenden Düsen- und Turbinenstömungen*, Dissertation, Universität Karlsruhe (TH), (in German), 1999

Hill, P. G.: Condensation of water vapour during supersonic expansion in nozzles, *J. Fluid Mech.*, 25:593–620, 1966

Hughes, F. R.; Starzmann, J.; White, A. J.; Young, J. B.: A Comparision of Modeling Techniques for Polydispersed droplet spectra in Steam Turbines, *Trans. ASME, J. Eng. Gas Turb. Power*, 138(4), 2015

IAPWS,: *Revised Release on Surface Tension of Ordinary Water Substance*, Internet resource, 2014

IAPWS-95,: *Revised Release on the IAPWS Formulation 1995 for Thermodynamic Properties of Ordinary Water Substance for General and Scientific Use*, Internet resource, 2014

IAPWS-IF97,: *Revised Release on the IAPWS Industrial Formulation 1997 for Thermodynamic Properties of Water and Steam*, Internet resource, 2007

Ihm, S. W.; Kim, C.: Computations of Homogeneous-Equilibrium Two-Phase Flows with Accurate and Efficient Shock-Stable Schemes, *AIAA J.*, 46(12):3012–3037, 2008

Kantrowitz, A.: Nucleation in Very Rapid Vapor Expansions, *J. Chem. Phys.*, 19(9):1097–1100, 1951

Kim, C. H.; Park, J. H.; Ko, D. G.; Kim, D. I.; Kim, Y. S.; Baek, J. H.: Analysis on Steam Condensing Flow Using Non-Equilibrium Wet-Steam Model, *J. Comput. Fluids Eng.*, 20(3):1–7, (in Korean), 2015

Lamanna, G.: *On Nucleation and Droplet Growth in Condensing Nozzle Flows*, Dissertation, Technische Universität Eindhoven, 2000

Li, L.; Feng, Z.; Li, G.: Study on Effects of Spontaneous Condensation on Performance of Low Pressure Stages in a Steam Turbine, in: *Proc. of ASME Turbo Expo 2006: Power for Land, Sea and Air*, Barcelona, Spain, 08–11 May 2006

Moore, M. J.; Walters, P. T.; Crane, R. I.; Davidson, B. J.: Predicting The Fog-Drop Size In Wet-Steam Turbines, in: *Proc. of IMECHE Conf. Wet Steam 4*, Coventry, UK, 1973

Moses, C. A.; Stein, G. D.: On the Growth of Steam Droplets Formed in a Laval Nozzle Using Both Static Pressure and Light Scattering Measurements, *Trans. ASME, J. Fluids Eng.*, 100(3):311–322, 1978

Onischuk, A. A.; Purtov, P. A.; Baklanov, A. M.; Karasev, V. V.; Vosel, S. V.: Evaluation of surface tension and Tolman length as a function of droplet radius from experimental nucleation rate and supersaturation ratio: Metal vapor homogeneous nucleation, *J. Chem. Phys.*, 124(1):014506-1–014506-12, 2006

Patel, Y.; Patel, G.; Turunen-Saaresti, T.: Influence of turbulence modelling on non-equilibrim condensing flows in nozzle and turbine cascade, *Int. J. Heat and Mass Transfer*, 88:165–180, 2015

Peters, M.; Paikert, F.: Nucleation and growth rates of homogeneously condensing water vapor in argon from shock tube experiments, *Experiments in Fluids*, 7(8):521–530, 1989

Reynolds, W. C.: *Thermodynamic properties in SI: Graphs, tables, and computational equations for forty substances*, Dept. of Mechanical Engineering, Stanford University, 1979

Schiller, L.; Naumann, A.: Über die grundlegenden Berechnungen bei der Schwerkraftaufbereitung, *Zeitschrift des Vereines Deutscher Ingenieure*, 77:318–320, 1933

Schnerr, G. H.: Unsteadiness in condensing flow: dynamics of internal flows with phase transition and application to turbomachinery, *Proc. Inst. Mech. Eng. C, J. Mech. Eng. Sci.*, 219(12):1369–1410, 2005

Schuster, S.; Benra, F.; Dohmen, H.; König, S.; Martens, U.: Sensitivity Analysis of Condensation on Calculated Liquid Film Motion in Radial Turbines, in: *ASME Conf. Proc. Turbo Expo 2014*, Düsseldorf, Germany, 16–20 June 2014

Starzmann, J.: *Numerische Untersuchung der Zweiphasenströmung und Analyse von Nässeverlusten in Niederdruckdampfturbinen*, Dissertation, ITSM, Universität Stuttgart, (in German), 2015

Starzmann, J.; Hughes, F. R.; White, A. J.; Grübel, M.; Vogt, D. M.: Numerical Investigation of Boundary Layers in Wet Steam Nozzles, in: *ASME Conf. Proc. Turbo Expo 2016*, Seoul, South Korea, 13–17 June 2016

Št'astný, M.: *Condensation of steam in nozzles and turbine cascades*, Univerity of West Bohemia, Pilsen,Czech Republic, ISBN 978-80-261-0489-6, 2015

Wagner, W.; Pruß, A.: The IAPWS Formulation 1995 for the Thermodynamic Properties of Ordinary Water Substance for General and Scientific Use, *J. Phys. Chem. Ref. Data*, 31(2):387–535, 2002

Walters, P. T.: Optical measurement of water droplets in wet steam flows, in: *Proc. of IMECHE Conf. Wet Steam 4*, Coventry, UK, Paper C32/73, 1973

Wegener, P. P.: *Nonequilibrium Flows, Part I*, chap. 4, pp. 163–243, Marcel Dekker, Inc., ISBN 0-8247-1770-8, 1969

White, A. J.: Numerical Investigation of condensing steam flow in boundary layers, *Int. J. Heat and Fluid Flow*, 21:727–734, 2000

White, A. J.; Senoo, S.: *Advances in Steam Turbines for Modern Power Plants*, Elsevier, chap.: Analysis and Design of Wet Steam Stages, to be published, 2016

White, A. J.; Young, J. B.: Time-Marching Method for the Prediction of Two-Dimensional, Unsteady Flows of Condensing Steam, *AIAA J. Propulsion and Power*, 9(4):579–587, 1993

Wróblewski, W.; Dykas, S.; Gepert, A.: Steam condensing flow modeling in turbine channels, *Int. J. Multiphase Flow*, 35(4):498–506, 2009

Wu, X.; Li, L.; G., L.; Feng, Z.: Numerical Investigation of the Effect of Inlet Condition on Self-Excited Oscillation of Wet Steam Flow an a Supersonic Turbine Cascade, *Int. J. Numer. Meth. Fluids*, 60(12):1334–1350, 2009

Yamamoto, S. Daiguji H.: Higher-order-accurate upwind schemes for solving the compressible Euler and Navier-Stokes equations, *Computer and Fluids*, 22(2/3):259–270, 1993

Yamamoto, S.: Computation of practical flow problems with release of latent heat, *Energy*, 30(2–4):197–208, 2005

Yee, H. C.: Construction of Explizit and Implicit Symmetric TVD Schemes and Their Applications, *J. Comp. Phys.*, 68(1):151–179, 1987

Young, J. B.: The Spontaneous Condensation of Steam in Supersonic Nozzles, *PhysicoChemical Hydrodynamics*, 3(1):57–82, 1982

Young, J. B.: An Equation of State for Steam for Turbomachinery and Other Flow Calculations, *Trans. ASME, J. Eng. Gas Turb. Power*, 110(1):1–7, 1988

Young, J. B.: Two-Dimensional, Nonequilibrium, Wet-Steam Calculations for Nozzles and Turbine Cascades, *Trans. ASME, J. Turbomach.*, 114(3):569–579, July 1992

Young, J. B.; White, A. J.: Special Issue on the Baumann Wet Steam Conference, *Proc. IMechE, Part A: J. Power and Energy*, 228(2), 2014

Table A1: Grid resolutions and dimensions

Nozzle test	coarse (I×J×K)	medium (I×J×K)	fine (I×J×K)	super fine (I×J×K)	no. of elements 2D unstruct. DoSkoda	$x_{\min}$ (cm)	$x_{\max}$ (cm)
Moore	$250 \times 71 \times 71$	$400 \times 101 \times 101$	$600 \times 131 \times 131$		50,000	-10	50
Moses and Stein	$250 \times 61 \times 61$	$350 \times 91 \times 91$	$550 \times 121 \times 121$		20,000	-5	6.5
Mystery (2D)	$300 \times 1 \times 41$	$500 \times 1 \times 71$	$800 \times 1 \times 111$	$1200 \times 1 \times 161$	20,000	-15	35

Table A2: Numerical methods and settings

Solver description	Turbulence model	EOS	Additional properties	Droplet representation	Nucleation	Droplet growth
CAM – Cambridge University (Chandler et al., 2014)						
3D FV-RANS-solver, denstiy-based, cell-vertex method, explicit 1st order 'scree' scheme, spatial: central differences with artificial viscosity	Spalart-Allmaras and laminar	IAPWS-IF97	IAPWS	Eulerian-Eulerian mixture model, moment method	$J_{\mathrm{CL,NISO}}$ eq. (4)	Young eq. (8) $\alpha = 11$, $\beta = 0$
CTU – Czech Technical University Prague (Halama et al., 2010a,b)						
2D laminar FV-solver, density based, cell-vertex method, sym. splitting (Strang) for different time scales, convection-diffusion explicit 2nd order Lax-Wendroff with artificial viscosity, cond. part by two-stage 2nd order Runge-Kutta	Laminar	Simple EOS, see eq. (11), $c_p(T_{\mathrm{g}})$ acc. to Heiler (1999)	h_{fg}, λ_{g}, ρ_{f} all temp. dependent acc. to Heiler (1999), IAPWS for σ and T_{s}	Eulerian-Eulerian mixture model, moment method	$J_{\mathrm{CL,NISO}}$ eq. (4)	Young eq. (8) $\nu = 0.9$, $\beta = 0$
Doosan – Doosan Heavy Industry & Construction (Ihm and Kim, 2008)						
2D preconditioned FV-RANS-solver, density based, cell-centred, implicit LU-SGS method, spatial: Roe's FDS with 3rd order MUSCL scheme and MHIS limiter	SST	IAPWS-IF97	IAPWS	Eulerian-Eulerian mixture model, monodispersed	$J_{\mathrm{CL,NISO}}$ eq. (4)	Gy. eq. (6), implemented acc. to (Halama and Fořt, 2013)

DoSkoda – Doosan Skoda Power and West Bohemia University (Šťastný, 2015)						
2D in-viscid FV-solver for *triangular grids*, density based, cell-centred, explicit, Symmetric TVD scheme (Yee, 1987) for Euler eq., cond. part by Upwind scheme	Laminar	Simple EOS, see eq. (11)	SVUSS Běchovice lib. (former Czech research inst.)	Eulerian-Eulerian mixture model, moment method	J_{CL} eq. (1)	Gyarmathy eq. (6)
DuEs – Universität Duisburg-Essen (Schuster et al., 2014)						
Ansys CFX, 3D FV-RANS-solver, pressure based, cell-vertex method implicit 2^{nd} backward Euler, spatial: 2^{nd} central differences, turbulence eq. automatic blending between 1^{st} and 2^{nd} order	SST	IAPWS-IF97	IAPWS	Eulerian-Lagrangian source term model, polydispersed, slip Schiller and Naumann (1933)	$J_{\mathrm{CL,NISO}}$ eq. (4), new drops added in volume if $J > 10^{15}\,\mathrm{m^{-3}s^{-1}}$ $\sigma_{\mathrm{eff}} = 0.95\sigma$	Young eq. (8) $\nu = 0.0$, $\beta = 0.0$ no capillary effect: $T_{\mathrm{l}} - T_{\mathrm{g}} = \Delta T$
ITSM – Universität Stuttgart (Grübel et al., 2015)						
Ansys CFX, 3D FV-RANS-solver, pressure based, cell-vertex method, implicit 2^{nd} backward Euler, automatic blending between 1^{st} and 2^{nd} order TVD scheme	SST and laminar	IAPWS-IF97	IAPWS	Eulerian-Eulerian source term model, monodispersed	$J_{\mathrm{CL,NISO}}$ eq. (4),	Young eq. (8) $\alpha = 0.0$, $\beta = 0.0$
Lap – Lappeenranta University of Technology (Patel et al., 2015)						
Ansys Fluent, 3D RANS-solver, density based, cell-centred, explicit 3-stage Runge-Kutta, spatial: 2^{nd} order Upwind, Roe's FDS scheme	modified $k-\epsilon$, Patel (2015)	Virial gas equation of Young (1988)	T_{s}, ρ_{f} Reynolds (1979), σ from Yg. (1982), others Eckert (1972)	Eulerian-Eulerian source term model, monodispersed	$J_{\mathrm{CL,NISO}}$ eq. (4)	Hill eq. (10)
MoPo – Moscow Power Engineering Institute						
Ansys Fluent, 3D FV-RANS-solver, user-defined wet steam model implementation, pressure based, cell-centred, implicit scheme	mod. $k-\epsilon$, Avetissian et al. (2005)	IAPWS-IF97	IAPWS	Eulerian-Eulerian mixture model, monodispersed	$J_{\mathrm{CL,NISO}}$ eq. (4)	Yg. eq. (8) $\alpha = 5$, $\beta = 0.0$, for $T \approx T_{\mathrm{s}}$ acc. to Halama (2013)
POSTECH – Pohang University of Science and Technology (Kim et al., 2015)						
3D FV-RANS-solver, density based, cell-centred, Euler implicit time marching, spatial: van Leer's FVS and Roe's FDS, MUSCL scheme, central differences for viscous fluxes	Spalart-Allmaras	Simple EOS, see eq. (11)	Functions based on IAPWS, σ considers Tolman length δ (Onischuk et al., 2006)	Eulerian-Eulerian mixture model, monodispersed	$J_{\mathrm{CL,NISO}}$ eq. (4), σ with Tolman modification (Onischuk et al., 2006)	Hill eq. (10)

ShTurb – Shanghai Turbine Works Co. Ltd. (Wu et al., 2009)						
2D/3D FV-RANS-solver, density based, cell-centred, implicit Euler time marching, spatial: 2^{nd} TVD scheme	$k-\epsilon$ model	Virial gas equation of Young (1988)	IAPWS	Eulerian-Eulerian source term model, monodispersed	$J_{\text{CL,NISO}}$ eq. (4)	Young eq. (8) $\nu = 0.2$ $\beta = 2.0$
SUT – Silesian University of Technology (Wróblewski et al., 2009)						
3D FV-RANS-solver, density based, cell-centred, explicit Runga-Kutta, spatial: FDS method, 3^{rd} order MUSCL scheme, Upwind scheme with 1D Riemann solver for EOS	SST	IAPWS-IF97 locally approx. by eq. with one virial coeff.	IAPWS	Eulerian-Eulerian mixture model, monodispersed	$J_{\text{CL,NISO}}$ eq. (4)	Gyarmathy eq.(6)
Tohoku – Tohoku University (Yamamoto, 1993, 2005)						
2D FD-RANS-solver, density based, implicit LU-SGS method, spatial: Roe's approximate Riemann solver and TVD with 4^{th} order MUSCL scheme, central differences for viscous fluxes	SST	Simple EOS, see eq. (11)	$\sigma_{\text{eff}} = f_\sigma\,\sigma$, f_σ empirical factor, σ Peters and Paikert (1989) others IAWPS	Eulerian-Eulerian mixture model, monodispersed	$J_{\text{CL,NISO}}$ eq. (4)	Young eq. (8), α has been varied, $\beta = 2.0$
Xian – Xi'an Jiaotong University (Li et al., 2006)						
2D, laminar FD-RANS-solver, density based, cell-centred, 1^{st} order explicit, spatial: 2^{nd} order TVD scheme	Laminar	Virial gas equation of Young (1988)	σ from Yg. (1982), others curve fit of IAWPS	Eulerian-Eulerian source term model, monodispersed	$J_{\text{CL,NISO}}$ eq. (4) condensation coeff. $q_{\text{c}} = 100$	Young eq. (8) $\alpha = 9$, $\beta = 2.0$, $q_{\text{c}} = 100$

FD = Finite Difference
FDS = Flux Difference Splitting
FV = Finite Volume
FVS = Flux Vector Splitting
LU-SGS = Low-Upper Symmetric Gauss-Seidel method
TVD = Total Variation Diminishing
MHIS = Multi-dimensional High Order Interpolation Scheme
MUSCL = Monotonic Upstream-Centered Scheme for Conservation Laws

$$p = \frac{(\gamma-1)(1-y)}{1+y(\gamma-1)}\left[e - \frac{1}{2}\varrho(u^2+v^2+w^2) + \rho y h_{\text{fg}}\right] \qquad (11)$$

y ... wetness fraction
e ... total energy of the mixture
ϱ ... mixture density